14. Kozono, D., Yasui, M., King, L. S. & Agre, P. (2002) *J. Clin. Invest.* **109,** 1395–1399.
15. Yasui, M., Kwon, T. H., Knepper, M. A., Nielsen, S. & Agre, P. (1999) *Proc. Natl. Acad. Sci. USA* **96,** 5808–5813.
16. Ma, T., Frigeri, A., Skach, W. & Verkman, A. S. (1993) *Biochem. Biophys. Res. Commun.* **197,** 654–659.
17. Ma, T., Yang, B., Umenishi, F. & Verkman, A. S. (1997) *Genomics* **43,** 387–389.
18. Harris, W. E., Akhavan, D., Miercke, L. J. & Stroud, R. M. (2004) *Proc. Natl. Acad. Sci. USA* **101,** 14045–14050.
19. Preston, G. M., Carroll, T. P., Guggino, W. B. & Agre, P. (1992) *Science* **256,** 385–387.
20. MacKinnon, R. (2004) *Angew. Chem. Int. Ed.* **43,** 4265–4277.
21. Agre, P. (2004) *Angew. Chem. Int. Ed.* **43,** 4278–4290.
22. de Groot, B. L. & Grubmuller, H. (2001) *Science* **294,** 2353–2357.
23. Tajkhorshid, E., Nollert, P., Jense, M. O., Miercke, L. J., O'Connell, H., Stroud, R. M. & Schulten, K. (2002) *Science* **296,** 525–530.
24. Smith, S. S., Steinle, E. D., Meyerhoff, M. E. & Dawson, D. C. (1999) *J. Gen. Physiol.* **114,** 799–817.

Fibroblast Growth Factor-2 Induces Recovery of Pulmonary Blood Flow in Canine Emphysema Models*

Shigeyuki Morino, MD; Tatsuo Nakamura, MD; Toshinari Toba, MD; Mitsuru Takahashi, MD; Toshihiro Kushibiki, MD; Yasuhiko Tabata, MD; and Yasuhiko Shimizu, MD

Study objectives: **Fibroblast growth factor (FGF)-2 is one of the most powerful angiogenic growth factors to be evaluated as an agent for the promotion of angiogenesis. The aim of this study is to investigate whether intratracheal administration of controlled-release FGF-2 microspheres restores pulmonary function in beagle dogs with emphysema.**
Design: **Randomized, controlled, experimental animal study.**
Subjects: **Eighteen Wister rats and 15 adult beagle dogs.**
Methods: **In the rat study, we compared the time profiles of the radioactivity remaining after intratracheal injection of ^{125}I-labeled FGF-2, either incorporated with the controlled-release microspheres or as an aqueous solution. In the dog study, elastase-induced emphysema models were developed in 10 animals, classified into the following three groups: control group (n = 5), emphysema model with empty microspheres-treated group (FGF − group, n = 5), and emphysema model with FGF-2 containing microspheres-treated group (FGF + group, n = 5).**
Results: **In the rat study, controlled-release microspheres maintained higher whole-lung FGF-2 concentrations after intratracheal administration. In the dog study, Pao_2 in the FGF + group was significantly higher than in the FGF − group after treatment. Pulmonary perfusion dynamic MRI revealed significant improvement in the signal intensity of damaged lung with the FGF + group. Linear intercept of the FGF + group was significantly reduced than the FGF − group.**
Conclusion: **Results indicate that intratracheal administration of FGF-2 induced an increase in pulmonary blood flow in the damaged lung and led to recovery of pulmonary function. The controlled-release microsphere system increased the effectiveness of FGF-2.**
(CHEST 2005; 128:920–926)

Key words: angiogenesis; COPD; emphysema; fibroblast growth factor; regeneration

Abbreviations: FGF = fibroblast growth factor; FGF − group = emphysema model with empty microspheres-treated group; FGF + group = emphysema model with FGF-2 containing microspheres-treated group; Lm = mean linear intercept; P/V = pressure/volume; LVRS = lung volume reduction surgery

Lung volume reduction surgery (LVRS) improves lung function, exercise capacity, and quality of life in patients with advanced emphysema by allowing the remaining pulmonary parenchyma and the respiratory muscles to function more effectively. Although the physiologic and symptomatic benefits of LVRS have, on average, been impressive, the substantial rates of morbidity and mortality associated with major thoracic surgery and general anesthesia in an elderly, debilitated population have limited the clinical utility of the procedure. Moreover, patients with the most advanced disease have higher surgical mortality, suggesting that LVRS is not suitable for those with severe disease.[1,2] There is currently no therapy for the treatment of lung emphysema. Noninvasive treatment is desirable for severe emphysema patients.

Fibroblast growth factor (FGF)-2 is one of the most powerful angiogenic growth factors to be evaluated as an agent for the promotion of angiogenesis. Patients with severe emphysema have higher-than-normal pulmonary arterial pressure. Severe emphy-

*From the Institute for Frontier Medical Sciences (Drs. Nakamura, Toba, Takahashi, Kushibiki, Tabata, and Shimizu), Kyoto University, Kyoto; and Division of Surgical Oncology (Dr. Morino), Nagasaki University School of Medicine, Nagasaki, Japan.
FGF-2 was provided by Kaken Pharmaceutical Company, Tokyo, Japan; and gadopentetate dimeglumine was provided by Magnevist, Nihon Schering, Osaka, Japan.
Manuscript received September 2, 2004; revision accepted January 3, 2005.

Correspondence to: Shigeyuki Morino, MD, Department of Bioartificial Organs, Institute for Frontier Medical Sciences, Kyoto University, 53 Kawaharacho, Shogoin, Sakyo-ku, Kyoto 606-8507, Japan; e-mail: morinos@frontier.kyoto-u.ac.jp

sema also tends to produce diffuse microvessel abnormalities in the pulmonary peripheral arteries.[3] Induction of a collateral pulmonary vessel network is a potent method of providing effective relief from dyspnea, general fatigue, and other symptoms in emphysema. Polymer hydrogels composed of gelatin have previously been demonstrated to be suitable matrices for the controlled release of growth factors because of their biosafety and the fact that they are highly inert toward protein drugs.[4] Biodegradable gelatin microspheres incorporating FGF-2 have been developed using acidic gelatin hydrogels. The use of these microspheres enables FGF-2 to be released at the site of action over a sufficiently long period of time to act effectively, in remarkable contrast to free FGF-2.[5] The aim of the present study was to investigate whether there is a benefit of bronchoscopic administration of FGF-2 on elastase-induced emphysema animals.

Materials and Methods

Distribution of FGF-2 Intratracheal Administration in Rats

Eighteen female Wister rats weighing 250 to 300 g and 15 adult beagle dogs weighing 10.0 to 14.9 kg were used in this study. The study protocol was approved by the Kyoto University Ethics Committee for Animal Research. All animals received humane care in compliance with the Principles of Laboratory Animal Care formulated by the National Society for Medical Research and the Guide for the Care and Use of Laboratory Animals prepared by the Institute of Laboratory Animal Resources, National Research Council, and published by the National Academy Press.

The rats were anesthetized with pentobarbital sodium, and the trachea was exposed. All the FGF-2 was labeled by ^{125}I. ^{125}I-labeled FGF-2 was injected via 0.3 mL of solution to the trachea (FGF solution group, n = 9). ^{125}I-labeled–FGF-2 microspheres were injected in 0.3 mL of suspended solution to the trachea (FGF microsphere group, n = 9). Lung tissues were obtained at different time intervals: 24 h, 72 h, and 7 days. The radioactivity remaining was calculated from the whole lung on a gamma counter (ARC-301B; Aloka; Tokyo, Japan).

Preparation of the Elastase-Induced Emphysema Model

The 15 beagle dogs were classified at random into the following three groups: control group, emphysema model with empty microspheres-treated group (FGF − group), and emphysema model with FGF-2 containing microspheres-treated group (FGF +) group. Models of elastase-induced emphysema were developed in the FGF − and FGF + groups. All interventions and physiologic measurements were performed under general anesthesia with ketamine hydrochloride (10 mg/kg) and xylazine (30 mg/kg), and mechanical ventilation was administered through an endotracheal tube. A 9.0-mm diameter endotracheal tube was inserted into the trachea under bronchoscopic guidance and attached to a mechanical ventilator. Continuous monitoring included ECG, oxygen saturation by reflectance oximetry using a sensor clipped to the ear, and body temperature by means of a rectal probe. A bronchoscope (5 mm outside diameter and 60 cm working length) was introduced through the indwelling endotracheal tube and advanced to the left segmental bronchus. Then, 40 mg (3,000 U) of porcine pancreatic elastase (Nakarai Tesque; Kyoto, Japan) was dissolved in 5 mL of saline solution and sprayed into all segmental bronchi of the left lung through the instrument channel of the bronchoscope using a spray infusion catheter (Olympus Optical; Tokyo, Japan) in the elastase-induced emphysema models. Each elastase dose was divided into 10 portions, each of which was sprayed in a different area to make a model of diffuse emphysema at the level of the left segmental bronchus. The right lung was preserved intact as a control.

Arterial Blood Gas and Pressure/Volume Relationships

Assessment of pulmonary function and MRI were performed before elastase administration (baseline), 4 weeks after elastase administration, and 4 weeks after treatment. For assessment of pulmonary function, dogs were anesthetized, intubated, and maintained on < 3.0% halothane. Arterial blood pH, $Paco_2$, Pao_2, and percentage of oxygen saturation were measured. Mechanical ventilation was set at a breathing frequency of 10 breaths/min, the inspiratory time was set to 33% of the breathing period, and the fraction of inspired oxygen was 0.2. Tidal volume was set to 18 mL/kg. Arterial blood gas samples were obtained from the right femoral artery 15 min after mechanical ventilation was started. A blood gas and acid-base analyzer (ABL-620; Radiometer; Copenhagen, Denmark) was used for measurements. Pressure/volume (P/V) relationships and expiratory capacity were also measured under general anesthesia with intubation. The intratracheal cavity was inflated to various pressures (5 to 70 cm H_2O), and the endotracheal tube was then clamped tightly. A plethysmograph (HI-701; Nihon Kohden; Tokyo, Japan) was connected to the endotracheal tube and the clamp was released, and then the expiratory capacity was measured. The expiratory capacity when the intratracheal cavity was inflated to a pressure of 40 cm H_2O (expiratory capacity, 40 cm H_2O) was used for calculations.

Dynamic Contrast-Enhanced MRI

All MRI studies were performed (1.5 T Sonata; Siemens Medical Systems; Erlangen, Germany) with a maximum amplitude of 40 mT/m and a rise time of 0.6 ms, using a phased-array body coil with four active segments. A turbo fast low-angle shot sequence optimized for projection imaging was used for dynamic contrast-enhanced MRI.[6] The following image parameters were used: echo time/repetition time, 1.35/350 ms; flip angle, 8°; readout bandwidth, 500 Hz/pixel; section thickness, 20 mm; field of view, 300 to 350 × 140 to 170 mm; image matrix, 110 × 256; and voxel size, 1.3 × 1.2 × 20.0 mm^3. For the MRI scan, each dog was anesthetized and a 16-gauge IV catheter was introduced into the right internal jugular vein. The dog was then fixed in a supine position and 3 mL of gadopentetate dimeglumine (Magnevist; Nihon Schering; Osaka, Japan) was administered as an IV bolus over 1 s. The contrast agent was administered immediately after the start of the dynamic imaging procedure. A total of 170 axial images were acquired to provide consecutive measurements over the 60-s scan time. The image immediately before the image showing any vascular enhancement was utilized as a mask image for subsequent image subtraction. For the imaging procedure, the signal intensity curves were measured from the right and left lung parenchymal areas (plotting area) separately. The mean signal intensity was calculated from the signal intensity curve during the 60-s scan time. The flow-volume ratio was calculated from the mean signal intensity of the left lung to the right lung, according to the following equation:

$$\text{Flow-volume ratio} = \frac{\text{mean signal intensity in left lung}}{\text{mean signal intensity in right lung}}$$

Administration of FGF-2 Microspheres

Human recombinant FGF-2 was supplied by Kaken Pharmaceutical Company, Tokyo, Japan. Gelatin was isolated from bovine bone collagen by an alkaline process using $CaOH_2$ (Nitta Gelatin Company; Osaka, Japan). FGF-2 microspheres with a diameter of approximately 10 μm were prepared as described previously by glutaraldehyde cross-linking of gelatin.[4,5] After washing with acetone (4°C), the microspheres were recovered by centrifugation. FGF-2 was radioiodinated and incorporated into the microspheres over a 1-h period before use. In the FGF + group, a total of 200 μg of FGF-2 was incorporated into each 4.0 mg of gelatin hydrogel microspheres. After performing a bronchoscopic examination, 4.0 mg of FGF-2 microspheres were suspended in 5 mL of saline solution and sprayed into the emphysematous left lung using a spray infusion catheter in 10 divided doses in a different area. The FGF − group were sprayed with 4.0 mg of gelatin hydrogel microspheres without FGF-2 using the same procedure into the left lung.

Histologic Measurement

Four weeks after treatment, the dogs in each group were euthanized by injection of pentobarbital sodium. The lung tissues and heart, along with the trachea, were resected *en bloc*. The heart and mediastinal tissues were removed, and the lungs with the attached trachea were weighed. The lungs were immediately inflated with 10% neutral buffered formalin solution via a tracheal cannula at a pressure of 25 cm H_2O until the pleura became tense. The trachea was then ligated, and the lungs were fixed further by immersion in formalin solution for 48 h. The inflated lung volume was measured by the water replacement method, and the left and right lungs were measured separately.[7] Twenty 2 × 2×2-cm blocks were randomly cut from the whole area of the lung per animal. The blocks were then embedded in paraffin before being cut into 3-μm-thick sections and stained with hematoxylin-eosin. All the sections were used to measure mean linear intercept (Lm), a commonly used stereologic indicator of alveolar airspace enlargement in emphysema, which was calculated as described.[8] Sixty fields per animal at 40 × magnification were chosen at random to measure Lm.

Statistical Analysis

Data are expressed as mean (SD). Data were analyzed by analysis of variance using statistical software (StatView for Windows, version 5.0; SAS Institute; Cary, NC). Differences between groups were identified by a Scheffe test; p values < 0.05 were considered statistically significant.

RESULTS

Distribution of FGF-2 Intratracheal Administration in the Rat

Figure 1 shows a summary of the FGF-2 remaining after intratracheal administration in the rats. Radioactivity remaining after intratracheal administration decreased with time. In the FGF solution group, radioactivity count remaining at 24 h, 72 h, and 7 days was 35.4 ± 3.6, 5.4 ± 2.5, and 1.2 ± 0.17, respectively. In the FGF microsphere group, remaining levels of FGF-2 were significantly higher than in the FGF solution group ($p = 0.003$). Radioactivity remaining at 24 h, 72 h, and 7 days was 50.2 ± 10.5, 13.7 ± 1.6, and 2.9 ± 1.63, respectively. These results suggest that the controlled-release microsphere system increased the effectiveness of FGF-2.

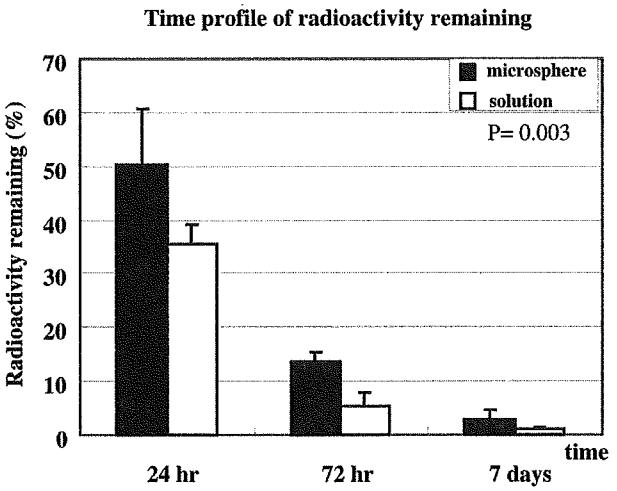

FIGURE 1. *In vivo* time profile of radioactivity remaining after intratracheal injection of gelatin microspheres incorporating ^{125}I-labeled–FGF-2 (microsphere) or intratracheal injection of ^{125}I-labeled–FGF-2 in aqueous solution (solution) into the rat trachea. In the FGF microsphere group, remaining levels of radioactivity were significantly higher than in the FGF solution group ($p < 0.01$). Data are presented as mean ± SD from nine rats per group at different time intervals: 24 h, 72 h, and 7 days.

Pulmonary Function Tests in the Canine Experiment

Body weights did not differ between the FGF − group and the FGF + group: 11.4 ± 1.3 kg vs 11.8 ± 1.9 kg, respectively. There were no differences in body weight 4 weeks after elastase administration and 4 weeks after treatment (FGF − group, 11.6 ± 1.2 kg vs 11.5 ± 1.5 kg; FGF + group, 11.5 ± 2.1 kg vs 11.0 ± 2.3 kg). There was no evidence of serious side effects, including thrombocytopenia, anemia, or renal dysfunction, after FGF-2 administration.

Data for PaO_2 are shown in Figure 2, *top*, *A*. There were no differences in any parameters between the two groups at baseline and 4 weeks after elastase administration: FGF −, 95.5 ± 7.3 mm Hg vs 85.5 ± 3.0 mm Hg; FGF +, 92.8 ± 4.2 mm Hg vs 88.7 ± 3.4 mm Hg, respectively. Elastase-induced emphysema models had significantly lower PaO_2 values at 4 weeks after elastase administration than at the baseline ($p = 0.015$). Four weeks after treatment, PaO_2 in the FGF + group was significantly higher than in the FGF − group: 83.7 ± 4.6 mm Hg vs 95.3 ± 5.9 mm Hg ($p = 0.036$).

The intratracheal cavity was inflated at different

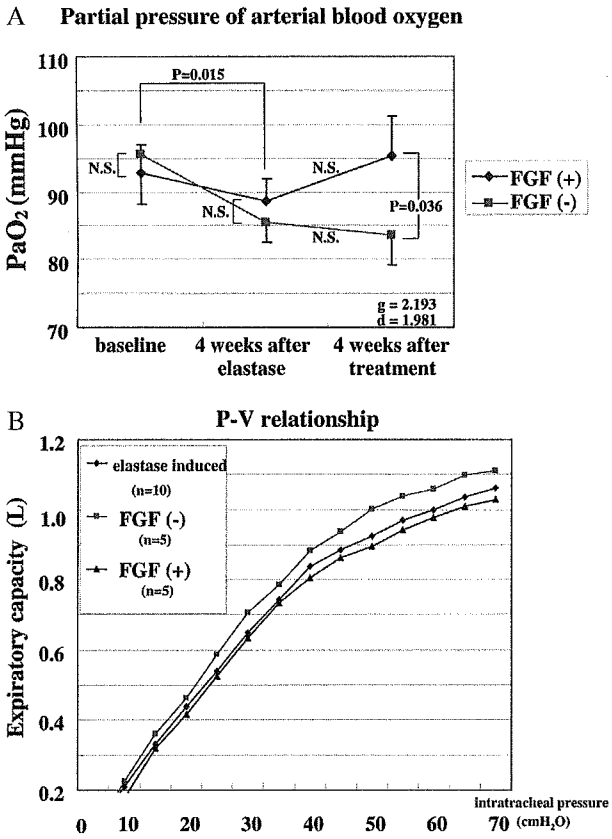

FIGURE 2. Results of pulmonary function tests in the FGF − group and the FGF + group. *Top, A*: Changes in PaO_2. Elastase-induced emphysema models had significantly lower PaO_2 values at 4 weeks after elastase administration than at baseline ($p = 0.015$). PaO_2 in the FGF + group was significantly higher than in the FGF − group at 4 weeks after treatment ($p = 0.036$). *Bottom, B*: The P/V relationship. The intratracheal cavity was inflated at different pressures (5 to 70 cm H_2O). Elastase-induced = elastase-induced emphysema models. The curve in the FGF − group was shifted upward to a greater extent than in the elastase-induced emphysema, whereas that in the FGF + group was shifted downward. N.S. = not significant.

pressures (5 to 70 cm H_2O). In the elastase-induced emphysema models, the P/V curve was shifted upward compared with the baseline. The curve in the FGF − group continued to shift upward, whereas that in the FGF + group shifted downward (Fig 2, *bottom, B*). The FGF + group appeared to exhibit better recovery than the FGF − group in terms of expiratory capacity with intratracheal pressure of 40 cm H_2O (0.88 ± 0.20 L vs 0.79 ± 0.18 L), although the difference was not statistically significant ($p = 0.72$). These results suggested pulmonary functional recovery in the FGF + group.

Dynamic Contrast-Enhanced MRI

MRI scans of pulmonary perfusion allowed the bolus of contrast agent to be followed through the superior vena cava, right atrium and ventricle, pulmonary arteries, lung parenchyma, pulmonary veins, left heart, and systemic arteries. At 5 s, the pulmonary arterial tree could be visualized beyond the segmental branches. A diffuse flash on the lung parenchyma was then observed, followed by a gradual increase in signal intensity over the next 20 s (Fig 3). In the elastase-induced emphysema models, the signal intensity was visually lower in the left lung. The left signal intensity was improved in the FGF + group. The difference between the left and right signals was maximal at 20 s. The signal intensity curves during the 60-s scan time are demonstrated in Figure 4. At the baseline, the levels of the signal intensity curves were the same in the right and left lungs. The signal intensity curve in the elastase-induced emphysema models declined in the left lung compared with the right (Fig 4, *top right, B*), and the signal intensity curve showed a sharply marked first-pass effect of enhancement with a significant lower-intensity peak on the pathologic side. The signal intensity curve in the FGF + group improved significantly in the left lung (Fig 4, *bottom right, C*). The flow-volume ratios at baseline were 0.99 ± 0.02 and 1.00 ± 0.04 in the FGF − group and the FGF + group, respectively (Fig 5). Four weeks after elastase administration, the flow-volume ratio was significantly lower than baseline: FGF − group, 0.70 ± 0.06; FGF + group, 0.69 ± 0.07. Four weeks after treatment, dynamic MRI revealed significant improvement in the FGF + group. The flow-volume

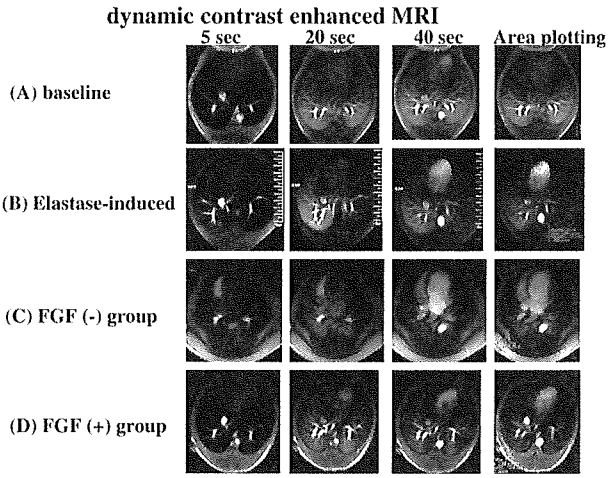

FIGURE 3. Dynamic contrast-enhanced MRI at baseline (*top row, A*), elastase-induced elastase-induced emphysema models (*upper center row, B*), the FGF − group (*lower center row, C*), and FGF + group (*bottom row, D*). At 5 s, the pulmonary arterial tree could be visualized beyond the segmental branches, followed by a gradual increase of signal intensity over the next 20 s. In the elastase-induced emphysema models, the signal intensity in the left lung was visually lower than that in the right lung. In the FGF + group, the signal intensity improved in the left lung, while the FGF − group showed no change.

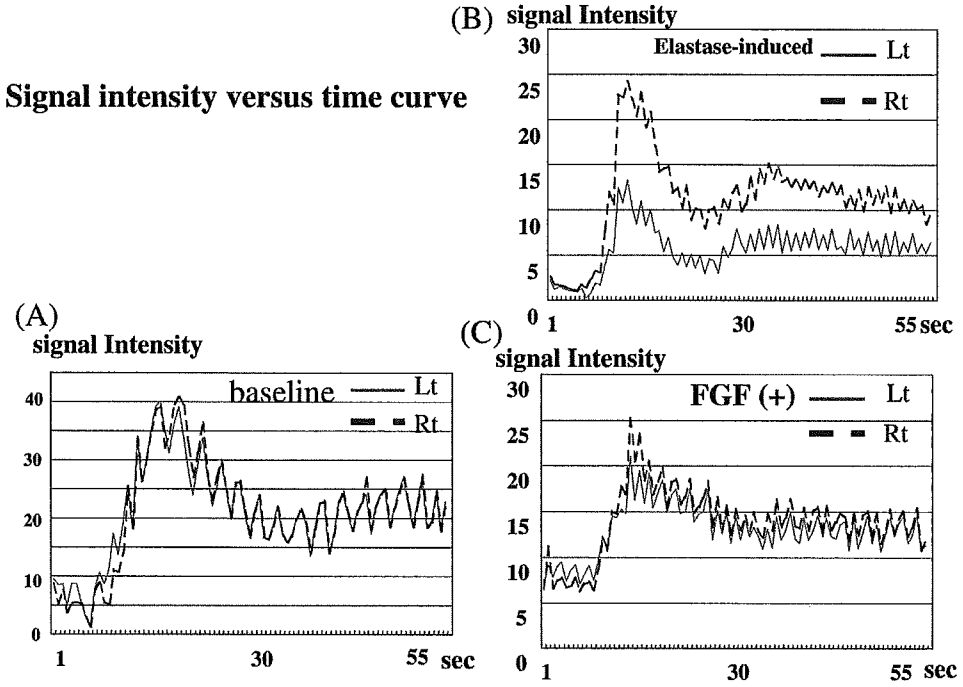

FIGURE 4. Signal intensity curves for the lung parenchyma (plotting area) after administration of gadopentetate dimeglumine during a 60-s scan time. *Left, A*: Baseline. The signal intensity curves for the left (Lt) and right (Rt) lungs were similar. *Top right, B*: Elastase-induced emphysema models. The signal intensity curve declined in the left lung compared with the right, and showed a sharply marked first-pass effect of enhancement with a significantly lower-intensity peak. *Bottom right, C*: FGF + group. Signal intensity curve was improved in the left lung.

ratio in the FGF + group was significantly improved after FGF-2 treatment, while the FGF − group score was the same as, or worse than, that in the dogs assessed before treatment: FGF −, 0.69 ± 0.05; FGF +, 0.88 ± 0.06 ($p = 0.0041$).

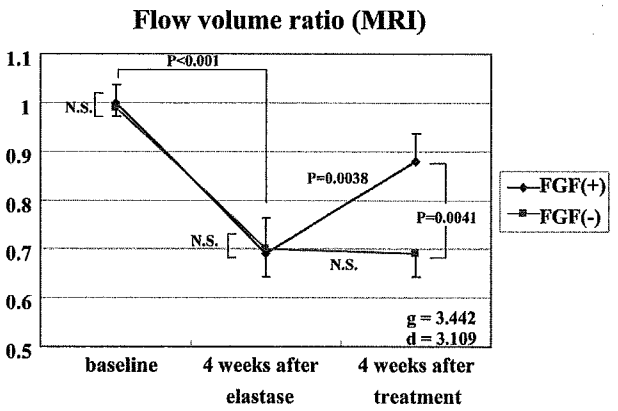

FIGURE 5. Flow-volume ratio determined by dynamic contrast-enhanced MRI. Four weeks after elastase administration, the flow-volume ratio was significantly lower than at baseline. The flow-volume ratio in the FGF + group was significantly improved after FGF-2 treatment, while the score for the FGF − group was the same as or worse than that for the dogs assessed before treatment. See Figure 2 legend for expansion of abbreviation.

Lung Volumes and Histologic Findings

A summary of the effects of FGF-2 on lung volume throughout the study period is presented in Figure 6. In the animals of the FGF − group, the left lung was overinflated compared with the control group. There were no changes in right lung volumes among the three groups. The left lung volume in the FGF + group was reduced compared to the FGF − group, although the difference was not statistically significant: control, 380.0 ± 82.9 cm^3; FGF −, 442.9 ± 50.4 cm^3; FGF +, 402.8 ± 71.8 cm^3. At autopsy, the tissue destruction caused by the elastase was associated with physiologic changes and a marked reduction in the surface area available for gas exchange (Fig 7). In the FGF + group, the mean size of alveoli was closer to control group than that of the FGF − group. There were no significant differences in right lung Lm levels among the three groups. Left lungs that had received elastase had a significantly increased Lm compared with the control group: control, 52.3 ± 2.8 μm; FGF −, 71.6 ± 4.0 μm; FGF +, 63.5 ± 3.2 μm. Lm levels in the control group and the FGF − group were significantly different ($p < 0.001$). The Lm value for the FGF + group appeared to indicate better recovery than in the FGF − group ($p = 0.02$).

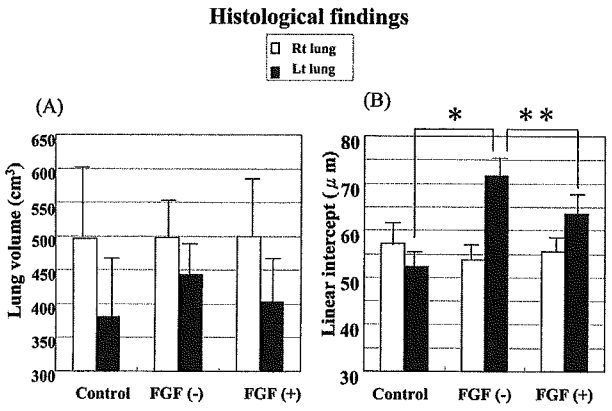

FIGURE 6. Histologic findings. *Left, A*: Lung volumes. *Right, B*: Linear intercept values. Left lung volumes in the FGF + group were reduced in comparison with the FGF − group. Left lungs that had received elastase showed significantly increased Lm values compared with those in the control group. *Lm levels in the control group and the FGF − group were significantly different from each other ($p < 0.001$). **The Lm value for the FGF + group appeared to indicate better recovery than in the FGF − group ($p = 0.02$). Rt lung = intact lung; Lt lung = treated lung.

DISCUSSION

Growth factors and biological regulators have been evaluated experimentally with respect to their potential usefulness in promoting pulmonary parenchymal regeneration in emphysema.[9–11] Reports[11,14] have suggested that growth factors play an important role in fetal lung development in both rodents and humans. FGF is a member of the heparin-binding polypeptide family. It is widely distributed and has been identified in many tissues of neuroectodermal and mesodermal origin. FGF acts as an angiogenic molecule *in vitro*, while *in vivo* it stimulates smooth muscle cell growth, wound healing, and tissue repair.[12] FGF-2 is one of the most powerful angiogenic factors known and is indispensable for lung development and branching morphogenesis. Studies[13,14] of the expression of FGF-2 and receptors in the developing fetal rat lung have shown that FGF-2 immunoreactivity is localized to cells of the airway epithelium, basement membranes, and extracellular matrix. However, although these characteristics of FGF-2 indicate that it would be a potent promoter of pulmonary functional recovery in emphysema, its biological half-life is reported to be < 50 min, which is too short a time to maintain a sustained response. In addition, endothelial cells take almost 1 day to begin to respond to FGF-2 stimulation.[15,16] Hence, the simple administration of free FGF-2 results in few of the desired biological activities such as angiogenesis, branching morphogenesis, and pulmonary functional regeneration. In fact, some researchers[17] have reported that FGF-2 administration produces insufficient angiogenesis to induce revascularization and subsequent airway healing. We used controlled-release microspheres as vehicles for more effective induction of angiogenesis by FGF-2.

When preparing microspheres, FGF-2 is incorporated into the hydrogel mainly as a result of physicochemical and electrical interactions between FGF-2 and the acidic gelatin, similar to the processes observed during hydrogen bonding and hydrophobic interactions.[4] Once incorporated, it is likely that the FGF-2 will be released from the gelatin hydrogel only when the hydrogel is enzymatically degraded to water-soluble gelatin fragments *in vivo*. A potential problem with this delivery system is therefore that FGF-2 release can only be controlled by changing the *in vivo* degradability of the gelatin hydrogels. This can be achieved by manipulating the water content of the hydrogels during their preparation.[4,5] We considered whether the microspheres could function as a drug delivery system in the airway and whether they had any unexpected side effects in the lung. In this *in vivo* study in rats, we compared the time profiles of the radioactivity remaining after intratracheal administration of ^{125}I-labeled–FGF-2 either incorporated with an acidic gelatin hydrogel or as an aqueous solution. The gelatin hydrogel yielded a higher radioactivity count than the aqueous solution, thus confirming the effectiveness of the gel as a controlled-release mechanism. The controlled-release microspheres expanded the effects of FGF-2 and prolonged its biological half-life *in vivo*. There was no evidence of serious complications including infection, atelectasis, allergy, and hemorrhage after

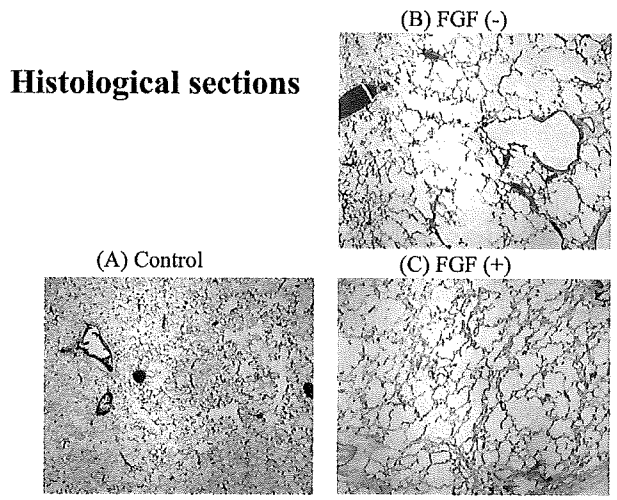

FIGURE 7. Representative photomicrographs of hematoxylin-eosin–stained sections (original × 40). *Left, A*: Control group; *top right, B*: FGF − group; and *bottom right, C*: FGF + group. The tissue destruction caused by the elastase was associated with physiologic changes and a marked reduction in the surface area. In the FGF + group, the mean size of alveoli was closer to the control group than that of the FGF − group.

gelatin hydrogels microspheres administration in this study. However, IV injection of hydrogels has a risk of vascular infarction. Therefore, gelatin microspheres cannot administer by the IV route.

Many groups have researched the lung parenchymal regeneration and alveolar septation for the chronic obstructive pulmonary diseases.[9,11,18] The mechanisms underlying regeneration and alveolar septation in the respiratory organs are still unclear, and it was not possible to determine whether FGF-2 treatment induced an increase in the number of alveoli or in alveolar septation. To date, we have found that FGF-2 treatment for COPD improves pulmonary function in the beagle dogs. The improvement in arterial oxygen gas data can be explained by the following: FGF-2 treatment led to a volume reduction in the affected lung and improvement of blood flow; subsequently, alveolar gas pressure also improved. Because oxygen uptake into the blood is dependent on the presence of a difference between the alveolar and capillary oxygen pressures, these improvements led to an improvement in the ventilation/perfusion shunt and in the gas exchange ability of the lung. In fact, little hypoxemia was observed after FGF-2 treatment, and the respiratory performance status of all dogs was improved, with no evidence of respiratory insufficiency.

There are some difficulties in attempting to achieve parenchymal regeneration and alveolar septation by the introduction of FGF-2 alone, because in the extracellular environment many growth factors and biological regulators interact with each other to produce parenchymal regeneration or alveolar septation.[13,19] It is difficult for tissue regeneration to occur in regions where blood flow is poor: pulmonary blood flow recovery is indispensable for lung regeneration and wound healing. Our present results indicate that the powerful angiogenic effect of FGF-2 induced both pulmonary revascularization and pulmonary vasodilation in the canine emphysema models, and suggest that this treatment may improve the symptoms of emphysema in humans. The magnitude of the physiologic improvement seen in response to FGF-2 treatment in this experimental model would be expected to benefit patients with severe emphysema to combine the intratracheal FGF-2 treatment and LVRS. We believe that intratracheal FGF-2 treatment has effective potential for emphysema, and that it will become one of the standard therapies for severe emphysema patients.

In conclusion, intratracheal administration of FGF-2 induced an increase in pulmonary blood flow in the damaged lung and volume reduction in the emphysematous lung. These changes led to an improvement in the ventilation/perfusion shunt and thus introduced the pulmonary functional recovery. The use of a controlled-release microsphere delivery system increased the effectiveness of FGF-2.

References

1 National Emphysema Treatment Trial Research Group. A randomized trial comparing lung-volume-reduction surgery with medical therapy for severe emphysema. N Engl J Med 2003; 348:2059–2073

2 National Emphysema Treatment Trial Research Group. Cost effectiveness of lung-volume-reduction surgery for patients with severe emphysema. N Engl J Med 2003; 348:2092–2102

3 Doi M, Nakano K, Hiramoto T, et al. Significance of pulmonary artery pressure in emphysema patients with mild-to-moderate hypoxia. Respir Med 2003; 97:915–920

4 Tabata Y, Hijikata Y, Muniruzzaman MD, et al. Neovascularization effect of biodegradable gelatin microspheres incorporating basic fibroblast growth factor. J Biomater Sci Polymer Edn 1999; 10:79–94

5 Yamamoto M, Ikada Y, Tabata Y. Controlled release of growth factors based on biodegradation of gelatin hydrogel. J Biomater Sci Polymer Edn 2001; 12:77–88

6 Hatabu H, Tadamura E, Levin DL, et al. Quantitative assessment of pulmonary perfusion with dynamic contrast-enhanced MRI. Magn Reson Med 1999; 42:1033–1038

7 Scherle W. A simple method for volumetry of organs in quantitative stereology. Mikroskopie 1970; 26:S57–60

8 Gillooly M, Lamb D, Farrow ASJ. New automated technique for assessing emphysema on histological sections. J Clin Pathol 1991; 44:1007–1011

9 Massaro GD, Massaro D. Retinoic acid treatment abrogates elastase-induced pulmonary emphysema in rats. Nat Med 1997; 3:675–677

10 Krause DS, Theise ND, Collector MI, et al. Multi-organ, multi-lineage engraftment by a single bone marrow-derived stem cell. Cell 2001; 105:369–377

11 Selman M, Cisneros-Lira J, Gaxiola M, et al. Matrix metalloproteinases inhibition attenuates tobacco smoke-induced emphysema in guinea pigs. Chest 2003; 123:1633–1641

12 Bikfalvi A, Klein S, Pintucci G, et al. Biological roles of fibroblast growth factor-2. Endocr Rev 1997; 18:26–45

13 Chabut D, Fischer AM, Colliec-Jouault S, et al. Low molecular weight fucoidan and heparin enhance the basic fibroblast growth factor-induced tube formation of endothelial cells through heparan sulfate-dependent α6 overexpression. Mol Pharmacol 2003; 64:696–702

14 Ambalavanan N, Novak ZE. Peptide growth factors in tracheal aspirates of mechanically ventilated preterm neonates. Pediatr Res 2003; 53:240–244

15 Lazarous DF, Schinowitz M, Shou M, et al. Effects of chronic systemic administration of basic fibroblast growth factor on collateral development in the canine heart. Circulation 1995; 91:145–153

16 Schaper W, De Brabander M, Lewi P. DNA synthesis and mitoses in coronary collateral vessels of the dog. Circ Res 1971; 28:671–679

17 Behrend M, von Wasielewski R, Klempnauer J. Failure of airway healing in an ovine autotransplantation model that includes basic fibroblast growth factor. J Thorac Cardiovasc Surg 2002; 124:231–240

18 Lucey EC, Goldstein RH, Breuer R, et al. Retinoic acid does not affect alveolar septation in adult FVB mice with elastase-induced emphysema. Respiration 2003; 70:200–205

19 Pepper MS, Vassalli JD, Orci L, et al. Biphasic effect of transforming growth factor β1 on *in vitro* angiogenesis. Exp Cell Res 1993; 204:356–363

Annals of Otology, Rhinology & Laryngology 114(12):907-912.

Destiny of Autologous Bone Marrow–Derived Stromal Cells Implanted in the Vocal Fold

Shin-ichi Kanemaru, MD, PhD; Tatsuo Nakamura, MD, PhD; Masaru Yamashita, MD; Akhmar Magrufov, MD; Tomoko Kita, PhD; Hisanobu Tamaki, MD; Yoshihiro Tamura, MD; Fuku-ichiro Iguchi, MD, PhD; Tae Soo Kim, MD; Masanao Kishimoto, MD; Koichi Omori, MD, PhD; Juichi Ito, MD, PhD

Objectives: The aim of this study was to investigate the destiny of implanted autologous bone marrow–derived stromal cells (BSCs) containing mesenchymal stem cells. We previously reported the successful regeneration of an injured vocal fold through implantation of BSCs in a canine model. However, the fate of the implanted BSCs was not examined. In this study, implanted BSCs were traced in order to determine the type of tissues resulting at the injected site of the vocal fold.

Methods: After harvest of bone marrow from the femurs of green fluorescent transgenic mice, adherent cells were cultured and selectively amplified. By means of a fluorescence-activated cell sorter, it was confirmed that some cells were strongly positive for mesenchymal stem cell markers, including CD29, CD44, CD49e, and Sca-1. These cells were then injected into the injured vocal fold of a nude rat. Immunohistologic examination of the resected vocal folds was performed 8 weeks after treatment.

Results: The implanted cells were alive in the host tissues and showed positive expression for keratin and desmin, markers for epithelial tissue and muscle, respectively. The implanted BSCs differentiated into more than one tissue type in vivo.

Conclusions: Cell-based tissue engineering using BSCs may improve the quality of the healing process in vocal fold injuries.

Key Words: bone marrow–derived stromal cells, cell-based tissue engineering, destiny of implanted cells, mesenchymal stem cells, regeneration, vocal fold.

INTRODUCTION

Damaged tissues and organs do not naturally regenerate, because rapid growth of fibroblasts and/or epithelial cells generally robs them of space for regeneration. This natural course also holds true for the repair process of an injured vocal fold. After vocal fold injury, the vocal fold may atrophy or form scar tissue. This process causes permanent sequelae of dysphonia and dysphagia. The primary treatment for these disorders is augmentation. Although various materials have been used for vocal fold augmentation, the ideal substance for injection has not yet been found.[1-7] Treatment by injection of space-filling materials remains unsatisfactory.

Mesenchymal stem cells (MSCs) are pluripotent cells that have the potential to differentiate into chondrocytes, osteoblasts, adipocytes, fibroblasts, bone marrow stroma, and other tissues of mesenchymal origin.[8-10] The MSCs are capable not only of differentiation along specific lineages, but also of being recruited to tissues in need, and are widely distributed throughout the body. The bone marrow stroma is considered the source of a common pool of multipotent cells that gain access via the circulation to various damaged tissues in need of repair.[11] Bone marrow–derived stromal cells (BSCs) are easily accessible from bone marrow aspirates and are an enriched source of MSCs. There is great optimism that BSCs can be used to engineer an unlimited source of cells for repairing damaged tissues and organs.

We previously reported that injured vocal folds could be regenerated by implantation of selectively cultured autologous BSCs and atelocollagen in an experimental canine model (Figs 1 and 2).[12] Im-

From the Department of Otolaryngology–Head and Neck Surgery, Graduate School of Medicine (Kanemaru, Yamashita, Magrufov, Kita, Tamaki, Tamura, Iguchi, Kim, Kishimoto, Ito), and the Department of Bioartificial Organs, Institute for Frontier Medical Sciences (Nakamura), Kyoto University, Kyoto, and the Department of Otolaryngology, Fukushima Medical University School of Medicine, Fukushima (Omori), Japan.

Presented at the meeting of the American Broncho-Esophagological Association, Boca Raton, Florida, May 13-14, 2005.

Correspondence: Shin-ichi Kanemaru, MD, PhD, Dept of Otolaryngology–Head and Neck Surgery, Graduate School of Medicine, Kyoto University, 54 Kawahara-cho, Syogoinn, Sakyo-ku, Kyoto 606-8507, Kyoto, Japan.

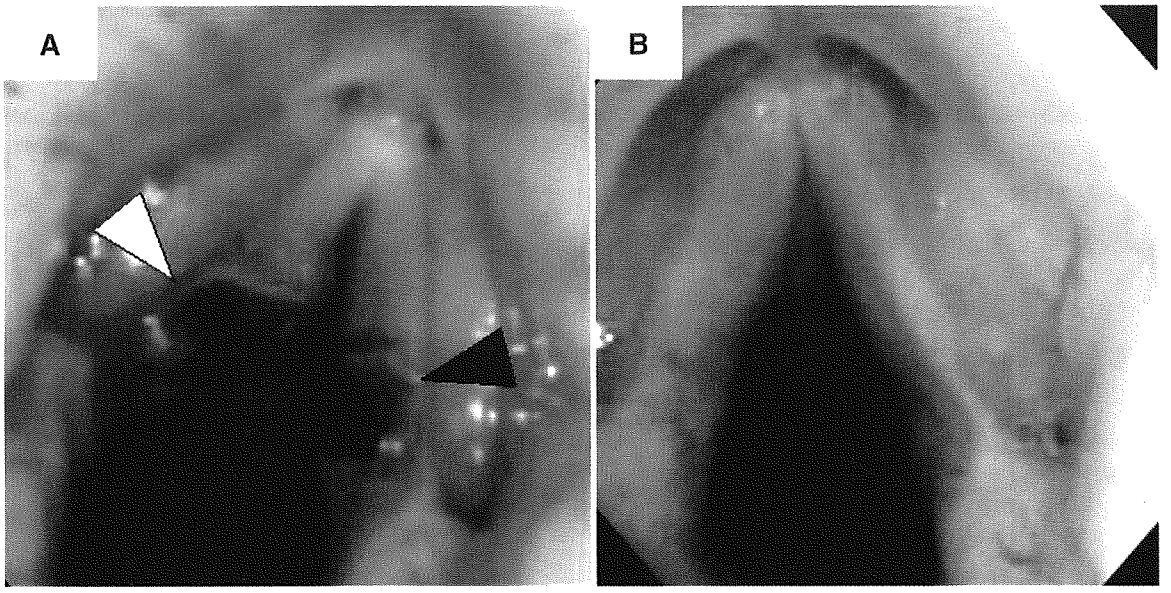

Fig 1. Morphological changes of vocal folds. **A)** Bilateral vocal folds were incised by electrocautery. Bone marrow–derived stromal cells (BSCs) with atelocollagen were implanted into left side of vocal fold (white arrowhead), and atelocollagen alone was injected into right side of vocal fold (black arrowhead). **B)** Morphological changes of injured vocal fold 2 months after treatment. Side with BSCs and atelocollagen implanted regenerated in almost normal shape, whereas atrophic changes occurred on side injected with atelocollagen alone.

planted BSCs undoubtedly play a key role in regeneration of the vocal fold; however, the fate of the implanted BSCs was not traced. Therefore, in this study, we focused on 2 issues: 1) characterization of cultured BSCs and 2) the types of host tissues derived from implanted BSCs.

MATERIALS AND METHODS

Animal Study. In this study we used 4 GFP (green fluorescent protein) transgenic mice and 4 nude rats. Animal care, housing, and surgery were in accordance with the Guidelines of the Animal Experiment Committee of Kyoto University. The animals were anesthetized with ether and intramuscular administration of ketamine hydrochloride (8.0×10^{-4} mg/g; Sankyo Co, Tokyo, Japan) and xylazine hydrochloride (5.0×10^{-4} mg/g; Bayer, Tokyo). Antibiotics were administered for control of postsurgical infection. All animals underwent the same procedure pattern from the time of harvest of autologous bone marrow until

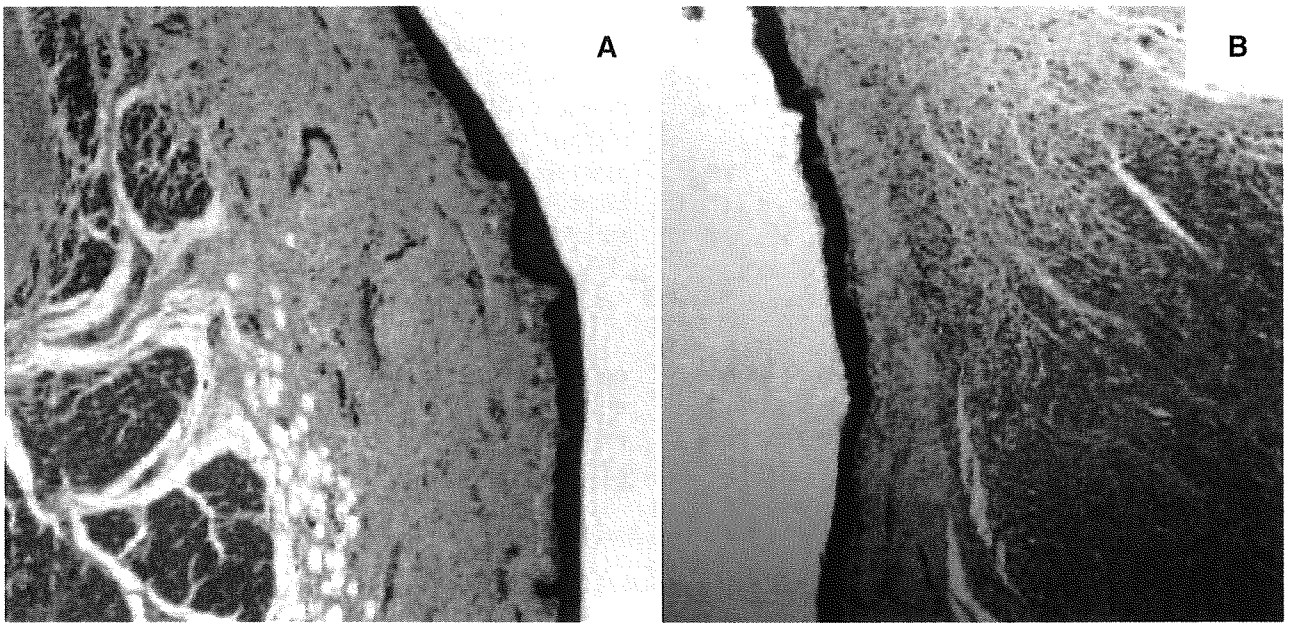

Fig 2. Vocal fold histology 2 months after treatment. **A)** BSCs with atelocollagen. Stratified structure of vocal fold is well regenerated. **B)** Atelocollagen alone. Scar formation between muscle and lamina propria is observed.

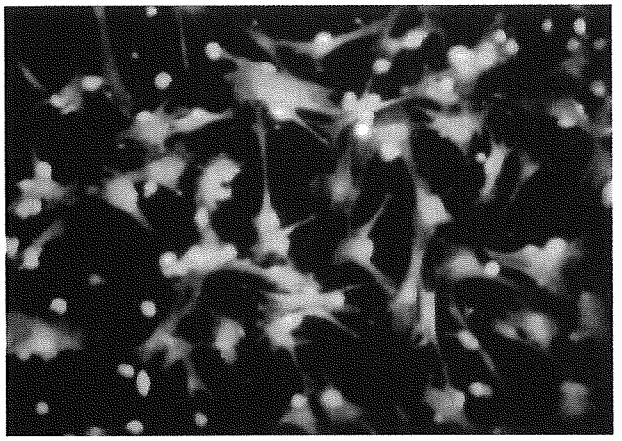

Fig 3. Fluorescent microscopic image of BSCs from GFP (green fluorescent protein) transgenic mouse 10 days after incubation.

they were painlessly sacrificed.

Harvest and Culture of BSCs. Under anesthesia, a GFP mouse was sacrificed and the bilateral femora were resected. By means of an injector with a 20-gauge needle, bone marrow was flushed from each femur and a single cell suspension was obtained. The bone marrow cells were placed in a 10-cm-diameter Petri dish with 15 mL of Dulbecco's modified Eagle's medium (DMEM) containing 10% fetal bovine serum and an antibiotic-antimycotic mixture (Gibco, Invitrogen Co, Carlsbad, California). The cells were incubated in 5% carbon dioxide at 37°C (MCO-17AIC carbon dioxide incubator, Sanyo Co, Osaka, Japan) for 48 hours in order to allow the BSCs time to adhere to the bottom of the dish. On day 3, the culture medium containing undesired floating contaminants, including hematopoietic cells and waste products, was removed to leave only adherent cells on the bottom of the dish (Fig 3). Fresh medium was then added and exchanged every 3 days. To amplify the number of BSCs, we continuously cultured cells for 14 days.

After 2 weeks, confluent growth of the cultured cells was confirmed microscopically (Olympus, IX70; Olympus Co, Tokyo) and the cells were detached from the bottom of the dish by addition of 2 mL of trypsin with 0.25% ethylenediaminetetraacetic acid (EDTA; Invitrogen Co). Approximately 2×10^6 to 6×10^6 cells were recovered from each plate. After neutralization of the trypsin solution, thorough washing of the cells with DMEM, and concentration by centrifugation at 3,500 rpm for 3 minutes (LX-120 centrifuge; Tomy Co, Tokyo), the cells were ready for injection or fluorescence-activated cell sorter (FACS) analysis.

Fluorescence-Activated Cell Sorter Analysis. The BSCs were cultured in control medium for 14 days before FACS analysis. The cells were stained with antibodies to Sca-1 (Ly-6A/E; eBioscience, San Diego, California), CD29 (Santa Cruz Biotechnology, Inc, Santa Cruz, California), CD34, CD44, CD45, CD49e, and 7-AAD (all from Becton Dickinson Biosciences, San Jose, California).

The MSCs were detached with trypsin-EDTA and counted. Approximately 1×10^5 cells were divided into aliquots in 5-mL centrifuge tubes and pelleted by centrifugation for 3 minutes at 400*g*. The cells were resuspended in 0.2 mL phosphate-buffered saline solution containing 1 mmol/L EDTA and 0.1% fetal bovine serum along with antibody combinations and incubated at room temperature for 20 minutes. Excess antibody was removed by washing. The cells were run on an FACS Calibur cytometer (Becton Dickinson and Company, Franklin Lakes, New Jer-

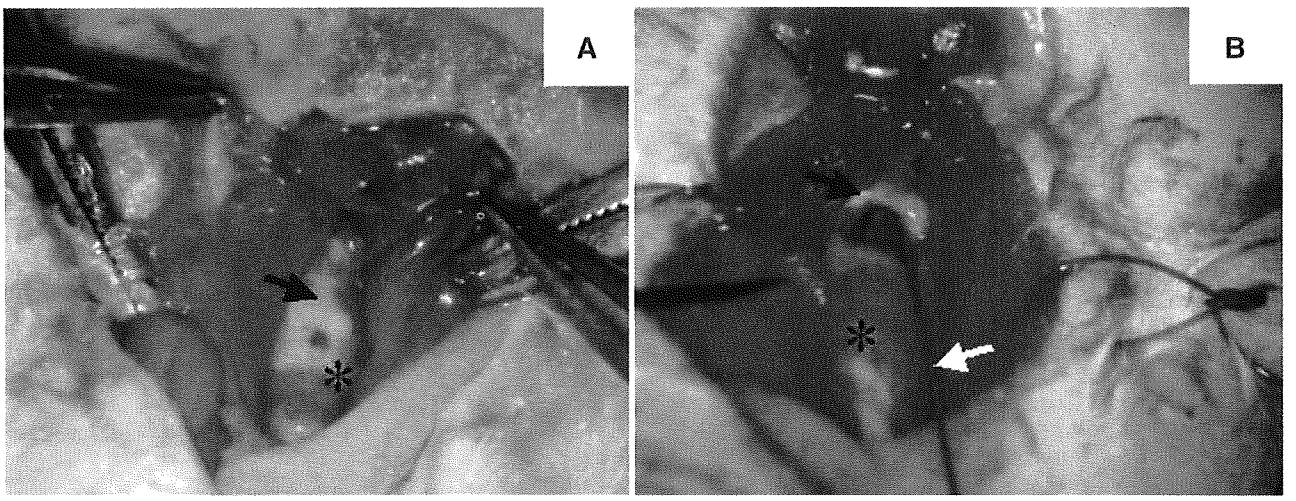

Fig 4. Surgical procedure. Black arrows — cricoid cartilage; asterisks — trachea. **A)** Vocal fold and surrounding tissues of nude rat are injured with 32-gauge needle through incision made at lower border of cricoid cartilage. **B)** BSCs from GFP mouse (1×10^5 to 3×10^5) are injected into damaged areas. White arrow — 32-gauge needle.

SURFACE ANTIGEN EXPRESSION OF BONE MARROW–DERIVED STROMAL CELLS

Surface Antigen	*Percent Positive*
CD29 (integrin β1)	>75
CD34	2-20
CD44	>75
CD45	2-20
CD49e (integrin α5β1)	20-75
Sca-1	>75

sey) and analyzed with Cell Quest software from a minimum of 1×10^4 collected events.

Surgical Procedures. Under anesthesia, a vertical skin incision was made on the neck of a nude rat and the larynx was exposed (Fig 4A). A half incision was made at the lower border of the cricoid cartilage, and the vocal fold and surrounding tissues were injured with a 32-gauge needle (Fig 4B). Fourteen-day cultured BSCs from a GFP mouse (1×10^5 to 3×10^5) were injected into the damaged areas with an injector with a 32-gauge needle. The incision was sutured with 6-0 Maxon (Ladary Japan, Tokyo). All surgical procedures were performed under a surgical microscope (Olympus OME KA-1; Olympus Co), and sterile techniques were used throughout the procedures. After surgery, all rats were given injectable antibiotics.

Histology. The nude rats were painlessly sacrificed 8 weeks after injury and BSC implantation. Immediately after sacrifice, the larynx and the upper part of the trachea were resected and fixed in 4% paraformaldehyde. Histologic examination consisted of an immunofluorescent technique using monoclonal antibodies (Cosmo Bio Co, Ltd, Tokyo) to keratin (epithelial cells) and desmin (muscle).

RESULTS

Phenotypic Characterization of BSC Populations. The expression of surface antigens on BSCs cultured for 14 days is shown in the Table. The BSCs expressed CD29, CD44, CD49e, and Sca-1, all markers for murine MSCs.[13] In addition, expression of

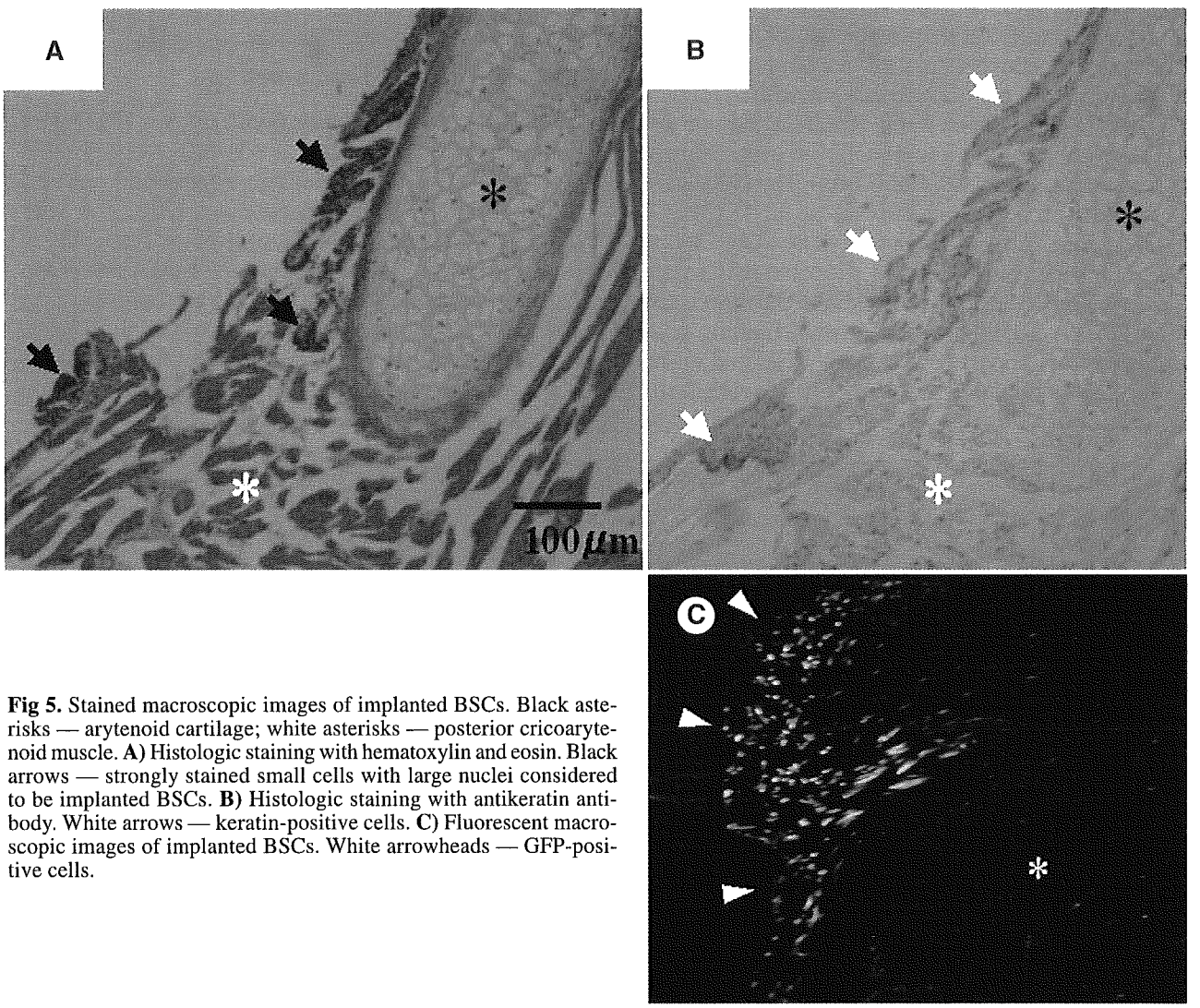

Fig 5. Stained macroscopic images of implanted BSCs. Black asterisks — arytenoid cartilage; white asterisks — posterior cricoarytenoid muscle. **A)** Histologic staining with hematoxylin and eosin. Black arrows — strongly stained small cells with large nuclei considered to be implanted BSCs. **B)** Histologic staining with antikeratin antibody. White arrows — keratin-positive cells. **C)** Fluorescent macroscopic images of implanted BSCs. White arrowheads — GFP-positive cells.

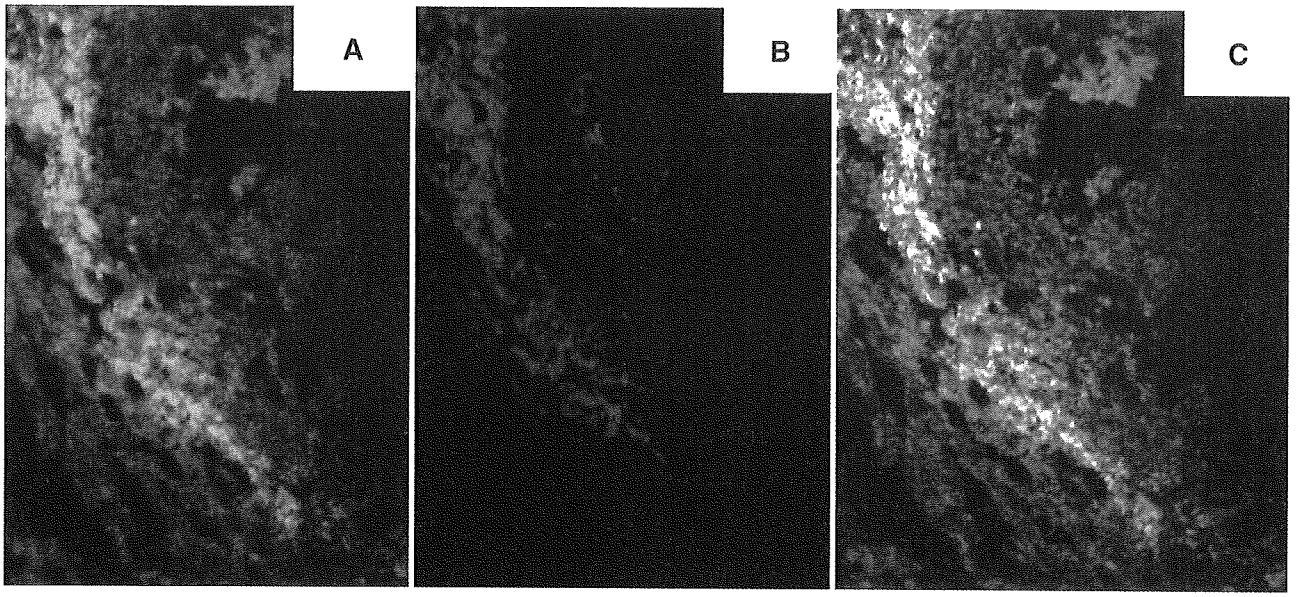

Fig 6. Fluorescent macroscopic images of implanted BSCs. **A)** GFP-positive cells. **B)** Desmin-positive cells. **C)** Composite of both images.

the hematopoietic lineage markers CD34 and CD45 was also observed in these cells.

Differentiation of Implanted BSCs in Nude Rats. All nude rats remained healthy during the observation period. In the lumen of the larynx, there were strongly stained small cells with a large nucleus (Fig 5A) that also stained for keratin (Fig 5B) and GFP (Fig 5C). These results demonstrate that BSCs from a GFP mouse differentiated into epithelial tissues in the peripheral regions of the vocal fold.

Cells positive for desmin were also found in the laryngeal lumen and mirrored the staining pattern of GFP (Fig 6). When the GFP and desmin staining patterns were merged, both desmin-positive and GFP-positive cells were observed, indicating that implanted BSCs differentiated into muscle cells. On the other hand, desmin-positive and GFP-negative cells were also observed in the same area, indicating the original host muscle cells. These results demonstrate that implanted BSCs differentiated into muscle cells in and around the original host muscle.

DISCUSSION

Stem cells are defined as a cell population that possesses self-renewal capacity and multilineage potential. There are many kinds of stem cells, including embryonic stem cells, MSCs, and neural stem cells. Embryonic stem cells have the largest potential and are the ideal source for therapeutic applications.[14,15] However, because embryonic stem cells are derived from the blastocyst inner cell mass, the issue of rejection is a concern, as are the multiple ethical and social concerns surrounding the use of embryonic stem cells. Thus, MSCs and BSCs have been proposed as an alternative source of stem cells.[11] The MSCs are described as multipotent, because of their ability to differentiate into a variety of different cells and tissue lineages. The BSCs are easily accessible via bone marrow aspirate and contain a rich source of MSCs that are easy to obtain and culture in vitro. Because these cells are autologous, there is neither rejection by the immune system nor the ethical problems encountered in the use of embryonic stem cells.

Although many studies have used MSCs derived from bone marrow, the cells are poorly characterized.[11,13] In this study, murine BSCs that were cultured for 14 days before implantation contained cells positive for the MSC surface markers CD29, CD44, CD49e, and Sca-1. In addition, expression of the hematopoietic lineage markers CD34 and CD45 was also observed in these cells, indicating that BSCs grown in this manner are composed of at least 2 lineage cell groups.

The vocal fold is composed mainly of 3 layers: the epithelial layer, the lamina propria, and the muscular layer. The lamina propria has the most important role in mucosal vibration. Although the atrophy and scarring that cause permanent dysphonia are observed primarily in this layer, they also occur in the other 2 layers. Therefore, for recovery of good phonation, it is insufficient to regenerate a single layer alone. This vocal fold tissue complexity makes treatment difficult.

Many treatments for vocal fold insufficiency have been reported.[1-7] The majority of these treatments include augmentation of the damaged vocal fold.

Various materials have been used for vocal fold augmentation, such as collagen, Teflon,[3] hyaluronic acid,[6] autologous fat,[4,5] and autogenous fascia.[7] However, simply injecting space-filling materials does not prevent vocal fold deformation. According to tissue engineering doctrine, a scaffold should be designed to encourage regeneration by cells residing at the site of transplantation. Collagen is a widely distributed extracellular matrix and a functionally essential component of vocal fold structure.[16,17] In our previous study, BSCs and atelocollagen were used as cells and as a scaffold, respectively. Although collagen is thought to be an ideal scaffold, it does not induce cellular regeneration in the damaged vocal fold; therefore, the vocal fold is unable to regenerate by transplantation of a scaffold alone. The success of regeneration depends on appropriate replenishment of cognate stem cells at the damaged site. From this viewpoint, BSC-based tissue engineering is essential for regeneration of the vocal fold.

Implanted BSCs undoubtedly play an important role in tissue regeneration. There is a possibility that BSCs directly differentiate into many kinds of tissues in vivo and/or stimulate host organs into regeneration. This study demonstrated that a portion of implanted BSCs could differentiate into 2 different tissue lineages — epithelial cells and muscle cells — in a damaged vocal fold and peripheral tissues. However, it remains to be determined whether implanted BSCs can differentiate into other tissues to work as a trigger for regeneration. Further studies are needed to determine the use of BSCs for clinical treatment.

CONCLUSIONS

In this study, we demonstrated that implanted BSCs were composed of at least 2 different lineage cell groups containing MSCs, and that they differentiated into 2 different tissue lineages in vivo: epithelial cells and muscle cells. It is possible that BSCs can be engineered as an unlimited source of cells to repair damaged complex tissues and organs such as the vocal fold.

Acknowledgments: The authors thank Satoshi Fujita for advice on fluorescence-activated cell sorter analysis and Dr Yoshinobu Toda for his histology expertise.

REFERENCES

1. Ford CN, Martin DW, Warner TF. Injectable collagen in laryngeal rehabilitation. Laryngoscope 1984;94:513-8.

2. Ford CN, Staskowski PA, Bless DM. Autologous collagen vocal fold injection: a preliminary clinical study. Laryngoscope 1995;105:944-8.

3. Trapp TK, Berke GS, Bell TS, Hanson DG, Ward PH. Effect of vocal fold augmentation on laryngeal vibration in simulated recurrent laryngeal nerve paralysis: a study of Teflon and Phonogel. Ann Otol Rhinol Laryngol 1989;98:220-7.

4. Mikaelian DO, Lowry LD, Sataloff RT. Lipoinjection for unilateral vocal cord paralysis. Laryngoscope 1991;101:465-8.

5. Brandenburg JH, Unger JM, Koschkee D. Vocal cord injection with autogenous fat: a long-term magnetic resonance imaging evaluation. Laryngoscope 1996;106:174-80.

6. Hallen L, Dahlqvist A, Laurent C. Dextranomeres in hyaluronan (DiHA): a promising substance in treating vocal fold insufficiency. Laryngoscope 1998;108:393-7.

7. Rodgers BJ, Abdul-Karim FW, Strauss M. Histological study of injected autologous fascia in the paralyzed canine vocal fold. Laryngoscope 2000;110:2012-5.

8. Pittenger MF, Mackay AM, Beck SC, et al. Multilineage potential of adult human mesenchymal stem cells. Science 1999; 284:143-7.

9. Deans RJ, Moseley AB. Mesenchymal stem cells: biology and potential clinical uses. Exp Hematol 2000;28:875-84.

10. Woodbury D, Schwarz EJ, Prockop DJ, Black IB. Adult rat and human bone marrow stromal cells differentiate into neurons. J Neurosci Res 2000;61:364-70.

11. Tuan S, Boland G, Tuli R. Adult mesenchymal stem cells and cell-based tissue engineering. Arthritis Res Ther 2003;5:32-45.

12. Kanemaru S, Nakamura T, Omori K, et al. Regeneration of the vocal fold using autologous mesenchymal stem cells. Ann Otol Rhinol Laryngol 2003;112:915-20.

13. Meirelles Lda S, Nardi NB. Murine marrow-derived mesenchymal stem cell: isolation, in vitro expansion, and characterization. Br J Haematol 2003;123:702-11.

14. Daley GQ, Goodell MA, Snyder EY. Realistic prospects for stem cell therapeutics. Hematology (Am Soc Hematol Educ Program) 2003:398-418.

15. Rippon HJ, Bishop AE. Embryonic stem cells. Cell Prolif 2004;37:23-34.

16. Sato K, Hirano M, Nakashima T. Fine structure of the human newborn and infant vocal fold mucosae. Ann Otol Rhinol Laryngol 2001;110:417-24.

17. Ishii K, Zhai WG, Akita M, Hirose H. Ultrastructure of the lamina propria of the human vocal fold. Acta Otolaryngol (Stockh) 1996;116:778-82.

日本臨床麻酔学会第23回大会シンポジウム

肺病変の修復・再生へのアプローチ

組織工学からみた臓器再生—気管・気管支の再生治療—

大森孝一[*1] 中村達雄[*2] 金丸眞一[*3]
安里 亮[*3] 山下 勝[*3] 清水慶彦[*2]

[要旨] 本研究の目的は，体内で自己組織の再生を誘導する *in situ* Tissue Engineering により，気道の臓器再生を実現することである．組織再生の足場としてポリプロピレンメッシュとコラーゲンスポンジから構成される人工材料を開発した．動物実験でこれを移植し最長5年の観察で，気管，主気管支，輪状軟骨の組織再生を確認した．これらの結果をふまえて，世界に先駆けて頸部気管で臨床応用を開始し，術後10ヵ月の時点で経過順調であった．しかし，胸部気管や分岐部気管ではまだ解決すべき問題は多い．今後は基礎実験の成果を臨床に橋渡しするトランスレーショナルリサーチにより，気道の各部位に応じた再生治療の開発が期待される．

キーワード：組織工学，気管・気管支，再生治療

（日臨麻会誌 Vol.25 No.3, 310～315, 2005）

はじめに

悪性腫瘍が気道に浸潤した例や気道の炎症性疾患，外傷例などで病変を切除した際，気道欠損部の再建が問題になる．気管・気管支は管状の枠組みを気管軟骨・気管支軟骨が保持しており，内腔面は気道という外界に接している．この構造を再建するためには，気道としての硬度をもった枠組みと内腔粘膜を，同時に再建する必要がある．従来，硬性組織には各種の軟骨，骨，人工材料などが，内腔面組織には皮膚や粘膜などが用いられたが[1),2)]，二期的にしかも他部位の手術が必要である．また，気管切除後の端々吻合術は，縫合不全の可能性や術後の挿管および頸部前屈体位など解決すべき問題点が残されている．

人工気管については，1960年代から数多くの研究が行われてきたが，現在までのところ臨床使用に耐えうる人工材料は開発されていない．唯一Nevilleらの人工気管が一時的に臨床応用されたが[3)]，気管断端との接合部の離開などの問題で現在は使われていない．Nakamuraらは1985年頃よりさまざまな人工気管を試作してきたが，1995年，自己組織が再生するようにデザインした人工材料を開発し，動物実験で良好な気管再生を実現できることを報告した[4)~6)]．さらに，同様の人工材料を輪状軟骨の切除後の欠損モデルに移植し，再生組織は正常と同等の硬さをもち，かつ良好な上皮化が得られることがわかった[7)]．

本研究グループでは，気道としての硬度をもった

[*1] 福島県立医科大学医学部耳鼻咽喉科学講座
[*2] 京都大学再生医科学研究所臓器再建応用分野
[*3] 京都大学大学院医学研究科耳鼻咽喉科・頭頸部外科学

著者連絡先 大森孝一
〒960-1295 福島市光が丘1
福島県立医科大学医学部耳鼻咽喉科学講座

枠組みと内腔粘膜を同時に再生させることを目的として，組織工学的手法による気管再生の研究を行っている．本稿では組織工学の考え方，人工材料の構造，動物実験における手術法や術後経過を述べ，最後に臨床応用に入った頸部気管の再生治療を紹介する．

Ⅰ　組織工学と臓器再生

臓器再生には足場，細胞，環境調節因子が必要で，この三要素に加えて血流が供給されると臓器再生が得られるとされている(**図1**)．

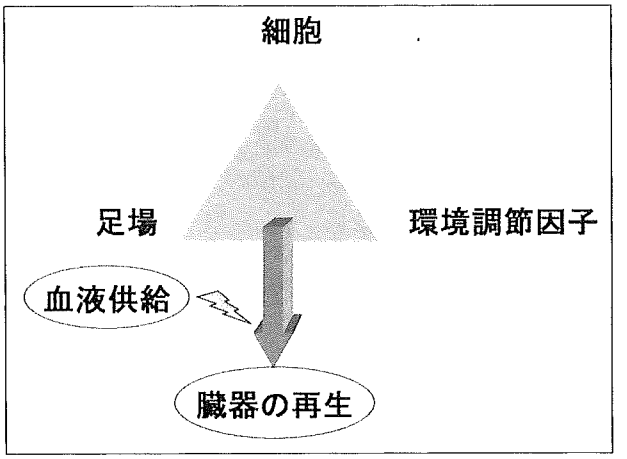

図1　臓器再生の三要素

組織工学(Tissue Engineering)は，工学的手法を使って細胞を二次元的，三次元的に組み上げ，本物の臓器や組織に近いものを再生させようというもので，VacantiとLangerら[8]によって始められた．彼らのTissue Engineeringは，体外で細胞を培養して目的とする組織をつくり，これを体内に移植する方法である．また，幹細胞や前駆細胞を移植することで組織再生を図ろうという研究が数多く行われているが，自己組織由来の細胞移植としては，循環器領域で下肢や心筋の血管再生を目指した血管内皮前駆細胞の移植[9]，整形外科領域で骨関節疾患の治療に骨髄間葉系幹細胞の移植[10]，眼科領域で角膜再生を目指して角膜上皮幹細胞を羊膜上で培養した移植などが行われている[11]．

一方，われわれの研究グループでは，体内の再生を目的とする臓器の場所で組織を再生させる*in situ* Tissue Engineeringという新しい概念に基づいて，1997年以後，動物実験で自己組織再生型の人工材料を移植し気管，輪状軟骨，食道，胃，小腸などが再生することを報告してきた[4)~7),12)~15)]．これらの実験では，細胞移植や増殖因子は使わずに足場の移植のみでの組織再生を行ってきた．

Vacantiらのように体外で組織を再生してから移植する方法や，自己組織由来であっても細胞移植を行うと，生きた細胞や組織を取り扱うことになるので，感染症対策や細胞の品質管理など臨床応用へのハードルが高い．これらの方法に比べて，われわれの行っている*in situ* Tissue Engineeringにより足場のみを移植する手法は安全性が高く臨床応用に近いといえる．気管，輪状軟骨までは，この方法である程度満足する成績が得られるものと思われる．解決すべき問題点としては，上皮化を加速する方法の開発，形態の複雑な喉頭，とくに声帯の再生などがあげられる．一方で，気道の臓器のなかで足場のみの移植では，難しい部位の組織再生を実現するには，将来的には幹細胞や前駆細胞の移植，増殖因子の投与も視野に入れた研究が必要であろう．

Ⅱ　人工材料

気管については管状の枠組みを保持するためポリプロピレン製のメッシュを管状にし，さらに同質の材料でリング状に補強し，組織再生の足場としてその周囲にコラーゲンスポンジを付加して，自己組織再生型の人工材料を開発した[4]．マーレックスメッシュは特定保険医療材料として従来から胸壁や腹壁の補強に臨床で使用されているもので，開発の過程で生体に取り込まれるメッシュの至適な編み目の大きさを決定し260μmとした．コラーゲンスポンジは医療用のブタ皮膚由来のⅠ型およびⅢ型コラーゲンを用いた．組織再生の良好な足場として近年，各領域でコラーゲンが使われている．本人工材料では，コラーゲンとメッシュがはずれにくいようにするた

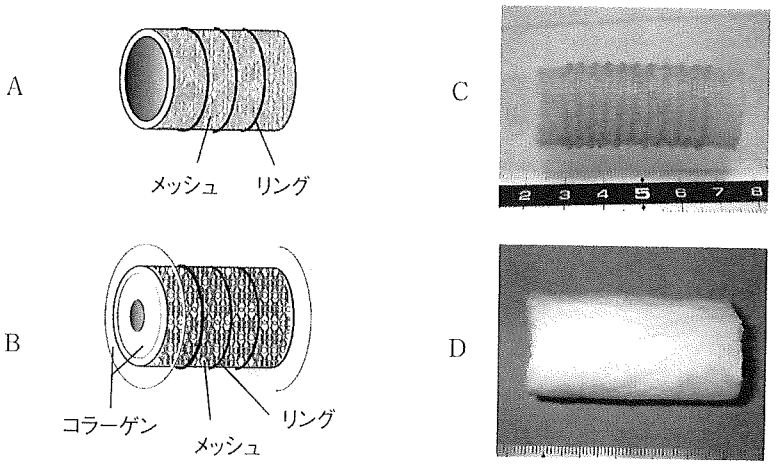

図2　人工材料
A，B：構造　C，D：外観

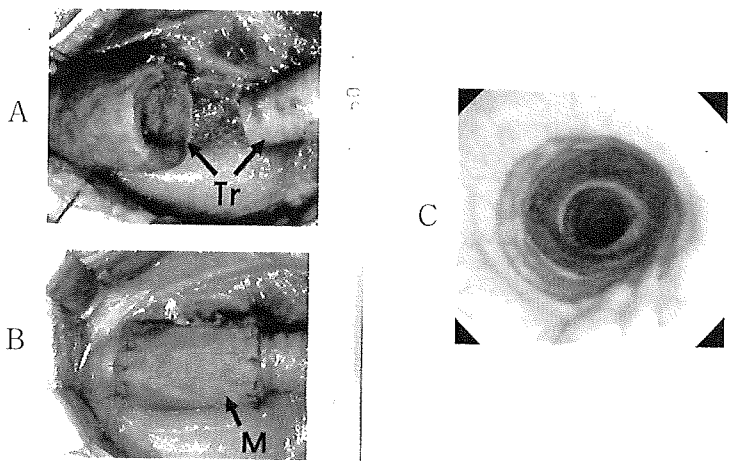

図3　動物実験（イヌ気管再生）
A：気管全周切除（Tr：気管）
B：人工材料の移植（M：人工材料）
C：術後1年の気管内視鏡所見

めに，コラーゲン液をメッシュ上に塗布したうえで，140℃，24時間の熱架橋を加えた．**図2**に人工材料の構造，外観を示す．輪状軟骨に対しては同様の材質で管腔状に加工した．気管分岐部・主気管支に対しては，同様の材質でY字型に加工した．

Ⅲ　動物実験

1. 気管・気管支

ビーグル犬を用い，全身麻酔下に頸部気管を露出した．長径約4cmを管状に全周切除し，そこに管状の人工材料を移植し，切除断端と吸収性糸で縫合した．手術法を**図3A，B**に示す．この際，人工材料は，再建気管の気密性を保つことと血液内の環境調節因子の働きを期待して，自己の血液でコラーゲンを湿潤させてから，断端組織を覆うようにして吸収性糸で縫合した．胸部気管では切除後に同人工材料を移植し，同様の方法で気管断端と縫合したうえで，血流と組織保護を期待して大網で被覆した[4]．

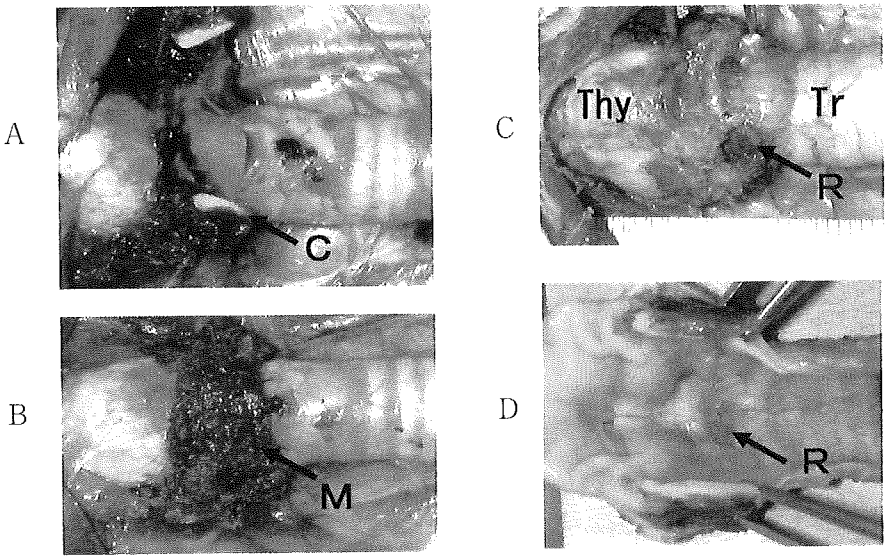

図4　動物実験（イヌ輪状軟骨再生）
A：輪状軟骨前半部切除（C：輪状軟骨）
B：人工材料の移植（M：人工材料）
C：術後4ヵ月の摘出喉頭の外観（R：再生組織，Thy：甲状軟骨，Tr：気管）
D：術後4カ月の摘出喉頭の内腔面（R：再生組織）
〔文献7）より改変〕

術後，組織学的評価を行うと，気管ではこのようにしてできた管状の組織管に，メッシュ内に結合織が入り込み，内腔面は再生した気管上皮で覆われ，電子顕微鏡で線毛を確認した．軟骨組織は再生しなかったが，再生気管の硬度については機械的圧縮試験を行ったところ，正常気管と同程度であった．少数例で肉芽やメッシュの露出を認めたが，いずれも軽度で呼吸には問題なかった[4]．正常気管との接合部にも安定した組織移行がみられ，長期にかつ安全に使用できることがわかった．術後1年の気管内視鏡所見を**図3C**に示す．最長5年の観察で，気管の上皮再生は良好であり問題なく経過している[5]．再建の困難な分岐部気管および主気管支には，Y字型に加工した本人工材料を移植すると，内面は完全に上皮化し気道の形状は保たれた．10例中8例で気管再生に成功したが，2例で感染が起こった．この部位での臨床応用には解決すべき問題が残されている[6]．

2. 輪状軟骨

ビーグル犬5頭に対して，輪状軟骨の前半部約1/2周を切除し，輪状軟骨欠損モデルとした[7]．さらに，ビーグル犬4頭に対して，輪状軟骨と気管を前半部約1/2周切除し，輪状軟骨・気管欠損モデルとした．自己組織再生型の人工材料を気管の場合と同様に作製し，その形状は円筒状で欠損範囲に応じて1/2周から2/3周を用いた．人工材料は，自己の血液でコラーゲンを湿潤させてから欠損部に合わせて形状を調整し，上方は甲状軟骨断端，下方は切除気管断端とを，吸収性糸で縫合した．輪状軟骨前半部の切除と人工材料の移植手術を**図4A，B**に示す．

術後3ヵ月～20ヵ月の観察で，内視鏡検査で全例が喉頭・気管の内腔面は上皮に覆われていた．全例で気道は十分保たれ，人工材料は生体組織内に取り込まれていた．2例で肉芽，1例でメッシュの露出を認めたが，いずれも軽度で呼吸には問題なかった．術後4ヵ月の摘出喉頭の外観と内腔からのマクロ像を**図4C，D**に示す．再生組織は上方の甲状軟骨，下方の気管輪と連続し，内腔面の上皮化がみられている．組織学的に評価すると，ポリプロピレンメッ

シュは周囲組織に取り込まれ異物反応を認めず，内腔面に線毛上皮の再生を認めた．機械的圧縮試験では，再生組織は正常組織と同等の支持力を示した．つまり，気道の枠組みと内腔上皮の両者を再生できたといえる．

これらのことから，自己組織再生型の人工材料は頭頸部癌の気道浸潤，声門下や気管の炎症性狭窄などにおける気管，輪状軟骨切除後の再建に臨床応用可能と考えられた．

Ⅳ 臨床応用

以上の動物実験の結果をふまえ，京都大学大学院医学研究科・医学部医の倫理委員会の承認を得て，ヘルシンキ宣言に則り本人工材料のヒトへの応用を開始した．甲状腺進行癌の気管浸潤例で十分に説明し，患者の同意を得たうえで本材料を使用した[15]．症例は79歳，女性．主訴は右頸部腫脹．CTにて甲状腺右葉全体を占める直径約5cmの腫瘍を認め，気管内視鏡では声門下に続く気管内腔の右側に隆起を認め，甲状腺腫瘍の気管浸潤が疑われた．

手術は，全身麻酔下に頸部襟状切開を加え，甲状腺腫瘍を露出した．甲状腺右葉は腫瘍で占拠され，頸部気管に癒着していた．癌組織の浸潤した頸部気管を安全域を含めて3気管輪，半周を切除した．その欠損部に本人工材料をトリミングして2/3周分の材料に自己の血液を注射器で注入し，気管欠損部をパッチする形で縫合した．術後2週間にはコラーゲンとメッシュが透見された．術後2ヵ月で上皮化し人工材料はほぼ被覆され，術後10ヵ月の時点で気管内腔面は上皮で覆われ，組織再生は良好な経過であった．

最後に

本稿では，体内で自己組織の再生を誘導する *in situ* Tissue Engineeringの考え方でわれわれが行っている気道再生について述べた．ポリプロピレンメッシュとコラーゲンスポンジから構成される足場材料を開発し，動物実験で気道の安定した組織再生が得られた．これらの結果をふまえて頸部気管で臨床応用を開始し，現時点では経過は順調である．しかしながら，気道の再生治療は始まったばかりであり，臨床成績を長期的に追跡して評価することが重要である．胸部気管や分岐部気管などでは動物実験の成績が安定しておらず，臨床応用にはまだ解決すべき問題が多く残されている．今後は，気道領域における再生医学研究が広まり，基礎実験の成果を臨床応用に結びつけるトランスレーショナルリサーチにより，気道の部位に応じた再生治療の開発が期待される．

本研究の一部は，平成15年度16年度 日本学術振興会基盤研究(B)(課題番号15390517)および平成16年度 厚生労働科学研究費補助金(ヒトゲノム・再生医療等研究事業)の助成を受けて行った．

参考文献

1) Cotton RT : Management of subglottic stenosis. Otolaryngol Clin North Am 33 : 111–130, 2000
2) Caputo V, Consiglio V : The use of patient's own auricular cartilage to repair deficiency of the tracheal wall. J Thorac Cardiovasc Surg 41 : 594–596, 1961
3) Neville WE, Bolanowski JP, Kotia GG : Clinical experience with the silicone tracheal prosthesis. J Thorac Cardiovasc Surg 99 : 604–613, 1990
4) Teramachi M, Kiyotani T, Takimoto Y, et al. : A new porous tracheal prosthesis sealed with collagen sponge. ASAIO J 41 : M306–310, 1995
5) Nakamura T, Teramachi M, Sekine T, et al. : Artificial trachea and long term follow–up in carinal reconstruction in dogs. Int J Artif Organs 23 : 718–724, 2000
6) Sekine T, Nakamura T, Matsumoto K, et al. : Carinal reconstruction with a Y–shaped collagen–conjugated prosthesis. J Thorac Cardiovasc Surg 119 : 1162–1168, 2000
7) Omori K, Nakamura T, Kanemaru S, et al. : Cricoid regeneration using in situ tissue engineering in canine larynx for the treatment of subglottic stenosis. Ann Otol Rhinol Laryngol 113 : 623–627, 2004
8) Langer R, Vacanti JP : Tissue engineering. Science 260 : 920–926, 1993

9) Asahara T, Murohara T, Sullivan A, et al. : Isolation of putative progenitor endothelial cells for angiogenesis. Science 275 : 964–967, 1997
10) Ohgushi H, Kitamura S, Kotobuki N, et al. : Clinical application of marrow mesenchymal stem cells for hard tissue repair. Yonsei Med J 45 (Suppl) : 61–67, 2004
11) Tsubota K, Satake Y, Kaido M, et al. : Treatment of severe ocular–surface disorders with corneal epithelial stem–cell transplantation. N Engl J Med 340 : 1697–1703, 1999
12) Yamamoto Y, Nakamura T, Shimizu Y, et al. : Intrathoracic esophageal replacement in the dog with the use of an artificial esophagus composed of a collagen sponge with a double–layered silicone tube. J Thorac Cardiovasc Surg 118 : 276–286, 1999
13) Hori Y, Nakamura T, Matsumoto K, et al. : Experimental study on in situ tissue engineering of the stomach by an acellular collagen sponge scaffold graft. ASAIO J 47 : 206–210, 2001
14) Hori Y, Nakamura T, Matsumoto K, et al. : Tissue engineering of the small intestine by acellular collagen sponge scaffold grafting. Int J Artif Organs 24 : 50–54, 2001
15) Omori K, Nakamura T, Kanemaru S, et al. : Regenerative medicine of the trachea : The first human case. Ann Otol Rhinol Laryngol (in press).

Tissue Engineering for Regeneration of the Trachea and Bronchus

Koichi OMORI*[1], Tatsuo NAKAMURA*[2], Shin–ichi KANEMARU*[3], Ryo ASATO*[3], Masaru YAMASHITA*[3], Yasuhiko SHIMIZU*[2]

*[1]Department of Otolaryngology, Fukushima Medical University School of Medicine
*[2]Department of Bioartificial Organs, Kyoto University Institute for Frontier Medical Sciences
*[3]Department of Otolaryngology–Head and Neck Surgery, Kyoto University Postgraduate School of Medicine

The present study demonstrates regeneration of the laryngeal and tracheal tissue using in situ tissue engineering technique for airway reconstruction. As the tissue scaffold, Marlex mesh reinforced with polypropylene rings covered by a collagen sponge was developed as the tissue scaffold. This scaffold material was implanted into the defect of the larynx and tracheas in beagle dogs. Post–operative endoscopy showed a well–epithelized surface of the subglottis and trachea. Based on the histological evaluations, regeneration of the cilial epithelium over the scaffold and good incorporation of the scaffold material into the host tissue were observed. Based on a mechanical test, the airway framework was firmly supported by the regenerated tissue. From the successful results of the experimental animal studies, the current regenerative technique was used to repair the trachea of a 78–year–old female patient with thyroid cancer. The right half of the three rings of the trachea was resected and the scaffold material was sutured to the defect. Epithelization continued to cover the artificial material completely for ten months without any complications. The current regenerative technique avoided tracheotomy, a second operation and cervical deformity. Although long–term observation is required, regenerative medicine of the tracheal tissue appears feasible to use for airway reconstruction.

Key Words : Tissue engineering, Trachea, Regenerative medicine